JOURNAL OF CATALYSIS 142, 552–560 (1993)

Determination of the Particle-Size Distribution of Iron Oxide Catalysts from Superparamagnetic Mössbauer Relaxation Spectra

BHASWATI GANGULY, F. E. HUGGINS, K. R. P. M. RAO, AND G. P. HUFFMAN[1]

Consortium for Fossil Fuel Liquefaction Science, 233 Mining and Mineral Resources Building, University of Kentucky, Lexington, Kentucky 40506

Received December 16, 1992; revised March 2, 1993

Mössbauer spectroscopy has been used to investigate the particle-size distribution of a variety of ultrafine iron-based direct coal liquefaction catalysts having either Fe_2O_3 or FeOOH composition. The Mössbauer spectra of these catalysts showed pronounced superparamagnetic relaxation effects. The relaxation spectra were analyzed as a function of temperature using a novel fitting model to determine the particle-size distribution for these catalysts. The resulting size distributions are in the nanometer range and agree reasonably well with size information obtained by scanning transmission electron microscopy (STEM), SQUID magnetometry, and X-ray diffraction (XRD).

INTRODUCTION

In recent years, there has been renewed interest in the use of iron-based catalysts for direct coal liquefaction (DCL) (*1–6*). In their as-prepared form prior to liquefaction, such catalysts are normally in the form of highly dispersed iron oxides and oxyhydroxides. The Mössbauer spectra of such fine iron oxide and oxyhydroxide particles exhibit pronounced superparamagnetic relaxation effects, which have been extensively investigated (*7–13*). Many of these studies of the superparamagnetic relaxation behavior of small particles have been based on an average particle volume or diameter (*7, 10–13*). Kundig *et al.* (*8*) were the first investigators to describe a method for determining the particle-size distribution of α-Fe_2O_3 by determining the percentage of the Mössbauer spectra in the form of magnetic hyperfine components as a function of temperature. We have used a similar technique to estimate particle-size distributions, with a novel model for fitting the Mössbauer spectra that incorporates a superparamagnetic component as well as magnetic hyperfine and quadrupole components.

EXPERIMENTAL PROCEDURES

Mössbauer spectra obtained in this study were obtained with a constant acceleration drive and spectrometer, similar to that described elsewhere (*14–16*), interfaced to a personal computer dedicated to data acquisition. Calibration spectra of metallic iron at room temperature were obtained simultaneously at the other end of the drive. Data were then transferred to a MicroVAX II computer for analysis and archival storage. The radioactive sources consisted of 25–100 mCi of ^{57}Co in a Pd matrix. Samples used in this study were prepared in powder form, diluted in boron nitride, if necessary, and mounted in plexiglass compression holders presenting a thin aspect to the gamma ray beam. Sample cooling to temperatures as low as 10 K was achieved using an Air Products Displex cryogenic system. In this system, the plexiglass sample holder was held between thin high-purity aluminum foil within a copper sample holder. Intermediate

[1] To whom correspondence should be addressed.

0021-9517/93 $5.00

temperatures between 10 K and room temperature were obtained using a small cartridge heater inserted in the copper sample block. The heat output of the cartridge heater to reach a specified temperature was adjusted electronically by means of a commercial temperature controller. The control-point temperature, equivalent to the sample temperature, was determined by means of a calibrated silicon diode inserted in the sample block and connected to the temperature controller.

The samples investigated include sulfated Fe_2O_3 and FeOOH prepared by a process discussed in detail elsewhere (*4*), Fe_2O_3 precipitated on carbon black (*17*), an ultrafine 30-Å Fe-oxyhydroxide catalyst developed by Mach I (*18*), and iron incorporated into lignite by cation exchange (*19*).

THEORY

When particles are small enough to behave superparamagnetically, the rapid relaxation of the particle spin system gives rise to complicated relaxation spectra which are superpositions of broadened magnetic hyperfine spectra, quadrupole doublets, and intermediate superparamagnetic (spm) spectra. The frequency, f, with which the coupled spins of a particle change direction is given by (*20*)

$$f = f_0 \exp\left(\frac{-K_a V}{kT}\right), \tag{1}$$

where K_a is the magnetic anisotropy constant, V is the particle volume, f_0 is a temperature insensitive constant frequency factor, k is Boltzmann's constant, and T is the temperature. The particle exhibits a six-peak magnetic hyperfine pattern when f is smaller than the nuclear Larmor frequency, f_L, of the ^{57}Fe nucleus, which is given by

$$f_L = \frac{g\beta H_0}{h}, \tag{2}$$

where g is the nuclear g value, β is the Bohr magneton, h is Planck's constant, and H_0 is the magnetic field at the ^{57}Fe site. When $f > f_L$, rapid spin relaxation causes the spectrum to gradually collapse into a quadrupole doublet.

To a first approximation, one can define a critical particle volume, V_c, above which a particle will exhibit a magnetic hyperfine spectrum. At temperature T, V_c is given by

$$V_c = \frac{kT}{K_a} \ln\left(\frac{f_0}{f_L}\right). \tag{3}$$

Kundig *et al.* (*8*) were the first to point out that an approximate size distribution could be determined by assuming that particles exceeding this critical volume gave rise to magnetic hyperfine spectra. Particle size distributions were then determined by measuring the magnetic percentages as a function of temperature. The difficulty with this approach is that the Mössbauer spectra are assumed to have sharp transitions from quadrupole doublets to magnetic sextets on lowering the temperature. It is well known, however, that this transition is gradual, occurring over a range of temperatures or relaxation times, τ ($\tau = 1/f$). Many papers have been written on the dependence of the shape of the Mössbauer spectra on the relaxation time (*21–23*). As shown by such authors as Wickman (*23*), the relaxation-time-dependent Mössbauer spectrum is given by

$$I(\omega) = \sum_{i=1}^{6} \frac{K_i[(1 + \tau\Gamma_i)P + QR]}{P^2 + Q^2}, \tag{4}$$

where P, Q, R for a zero external magnetic field have the form

$$\begin{aligned} P &= \tau[\Gamma_i^2 - (\Delta - \omega)^2 + \delta_i] + \Gamma_i \\ Q &= \tau(\Delta - \omega) \\ R &= (\Delta - \omega)(1 + 2\tau\Gamma_i) \\ \delta_i &= \tfrac{1}{2}(\omega_{7-i} - \omega_i), \quad \Delta = \tfrac{1}{2}(\omega_{7-i} + \omega_i), \end{aligned} \tag{5}$$

where τ is the relaxation time in sec, ω is the frequency (in sec^{-1}) corresponding to the Doppler energy of each data point in the Mössbauer spectrum, and ω_i are the frequencies (in sec^{-1}) corresponding to the six allowed transitions between the Zeeman

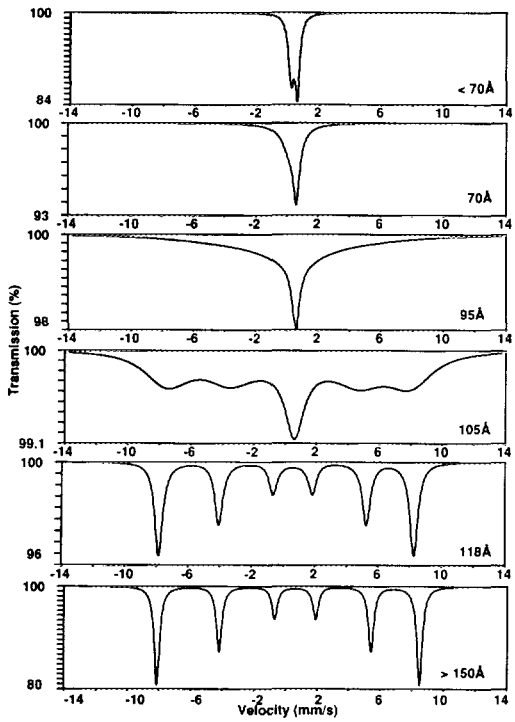

FIG. 1. Theoretical plots of relaxation spectra of Fe_2O_3 at room temperature as a function of particle size.

split energy levels. K_i are the Clebsch–Gordon coefficients with $K_6 = K_1 = 3$, $K_5 = K_2 = 2$, and $K_4 = K_3 = 1$ for zero external magnetic field. Γ_i is the natural line width in sec^{-1} and is taken to be the same for all transitions.

RESULTS AND DISCUSSION

Figure 1 shows the theoretical Mössbauer spectra of α-Fe_2O_3 as a function of size using the model given by Eqs. (4) and (5). In Eq.(5), the ω_i are calculated from the Mössbauer parameters of bulk α-Fe_2O_3 at room temperature. The particle size corresponding to each $\tau(= 1/f)$ is calculated from Eq. (1) assuming the particles to have a spherical shape. We have used the values of the magnetic anisotropy constant given by Van der Kraan (*11*) (0.55×10^5 J/M^3 for α-Fe_2O_3) and Rodmacq (*12*) (1.67×10^5 J/M^3 for α-FeOOH). Different authors have used different values for the parameter f_0 (*7, 8, 10–13, 24–26*), but it is always taken as a constant. The choice of f_0 depends on the material and the size ranges of particles studied. In the work of Van der Kraan (*11*) concerning superparamagnetic properties of fine α-FeOOH and α-Fe_2O_3 particles, the interval of possible values of f_0 is cited as 10^9 to 10^{12} sec^{-1}. For our studies concerning as-prepared and as-dispersed catalysts, the value of f_0 was determined empirically using the 30-Å FeOOH catalyst obtained from Mach I (*18*). A TEM investigation of this sample (*27*) showed that the particles were approximately spherical and had a narrow size distribution with an average particle diameter of 30 Å. The Mössbauer spectrum of this sample was taken at 10 K and was found to be simulated quite well using the superparamagnetic model described in Eq. (4) with a relaxation time (τ) of 10^{-7} sec. This value of relaxation time and the particle volume was substituted into Eq. (1) and a value of 10^{12} sec^{-1} was obtained for f_0, which was used to calculate the size distributions for all the samples studied here. It should be noted that the accuracy of f_0 is not very critical for this study, since changing f_0 by one order of magnitude shifts the size ranges by ± 5 Å only. Additionally, the value of f_0 used here is quite consistent with that used by other authors. Vertes *et al.* (*10*), for example, reported a value of $f_0 = 10^{12}$ sec^{-1} for δ-FeOOH particles of 30 Å diameter.

Using these parameters and Eq. (3), a critical diameter, $d_c = 115$ Å is derived for α-Fe_2O_3 at room temperature (295 K). It is seen in Fig. 1 that the theoretical spectrum calculated using Eq. (4) is indeed a six-peak magnetic hyperfine spectrum at this particle diameter, although it is slightly broadened. At a somewhat larger particle diameter, a sharp six-line magnetic hyperfine pattern with no significant broadening is seen. Figure 1 also shows that for decreasing particle size, the Mössbauer spectrum gradually collapses to a quadrupole doublet. It is seen that a sequence of superparamagnetic (spm) relaxation spectra that are neither magnetic

nor quadrupole in character occur as the particle-size decreases below the critical diameter. At a much smaller diameter (70 Å for α-Fe_2O_3 at 295 K), a pattern that could probably be described as a broadened, asymmetric quadrupole doublet emerges. As pointed out by Blume (*28*), the asymmetry in the quadrupole doublets seen in the Mössbauer spectra arises because the $\pm 3/2 \rightarrow \pm 1/2$ transitions, which make up one of the lines of the quadrupole doublet, narrow more slowly than the $\pm 1/2 \rightarrow \pm 1/2$ transitions, which make up the other line, since the precession frequency in the magnetic field is larger for $\pm 3/2 \rightarrow \pm 1/2$ transition.

At a given temperature, particles with a diameter exceeding some critical diameter, d_M (corresponding to Eq. (3)), will exhibit a magnetic hyperfine spectrum, while particles with a diameter less than some other critical value, d_Q, will exhibit a quadrupole doublet. Particles having diameters d such that $d_Q < d < d_M$ will exhibit spm relaxation spectra that are neither magnetic nor quadrupole in nature, as illustrated by the middle three spectra of Fig. 1. A typical iron oxide catalyst will normally have a size distribution such that, over some range of temperature, some particles fall into all three size classifications, yielding spectra that are a mixture of magnetic, quadrupole, and spm relaxation spectra. The situation is further complicated by the fact that iron atoms on or near the surface of particles exhibit somewhat different Mössbauer parameters from those in the particle interior (*9*). Nevertheless, we have developed a simple model for analyzing such spectra that gives least squares fits of acceptable quality and yields particle size distributions that are in good agreement with those obtained by other methods. The model consists of fitting the spectra with one or more magnetic hyperfine components corresponding to particles with $d \geq d_M$, one or more quadrupole components, representing particles with $d < d_Q$, and a single spm relaxation spectrum, representing particles for which $d_Q < d < d_M$. The magnetic and quadrupole components are fitted in the normal fashion (*14–16*), with the hyperfine fields, quadrupole splittings, isomer shifts, linewidths, and peak intensities as variables. Normally, two or three magnetic and one or two quadrupole componets were required.

From the values of the Mössbauer parameters for the magnetic and quadrupole components, the iron oxide is identified as having either an Fe_2O_3 or FeOOH structure. The spm component is then fitted with Eqs. (4) and (5), using values of ω_i calculated from the hyperfine field, isomer shift, and quadrupole parameters of either α-Fe_2O_3 or α-FeOOH. The spm component is fitted as a completely separate entity to the normal quadrupole and magnetic components within the least-squares program. The value of the natural linewidth, Γ (sec^{-1}) is entered manually. Although the value of Γ is a constant (1×10^7 sec^{-1} for ^{57}Fe), some adjustment of its value is necessary due to the approximate nature of the model. A Γ value between 1.2×10^7 and 1.5×10^7 sec^{-1} was found appropriate to fit most of the experimental data. The only variables for the spm component are the relaxation time, τ, and its amplitude relative to the other components. The starting value of τ can be estimated by first simulating the magnetic and quadrupole parts of the experimental spectrum, then comparing the difference to spm spectral shapes such as those in Figure 1. For most samples, a τ value between 10^{-9} and 10^{-10} sec was appropriate for the superparamagnetic component. A starting value of the relative amplitude of the superparamagnetic component is estimated visually.

Some examples of least squares fits obtained using this model are shown in Figs. 2 and 3. Figure 2a shows the room temperature spectrum of a sulfated Fe_2O_3 catalyst (6.1% $SO_4^=$) which has an α-Fe_2O_3 structure and Fig. 2b shows a room-temperature spectrum of a lignite coal, which was ion exchanged with Fe-acetate to yield ultrafine particles with α-FeOOH composition. Figures 3a and 3b show spectra obtained at 100 K of a sulfated Fe_2O_3 catalyst (2.1% $SO_4^=$;

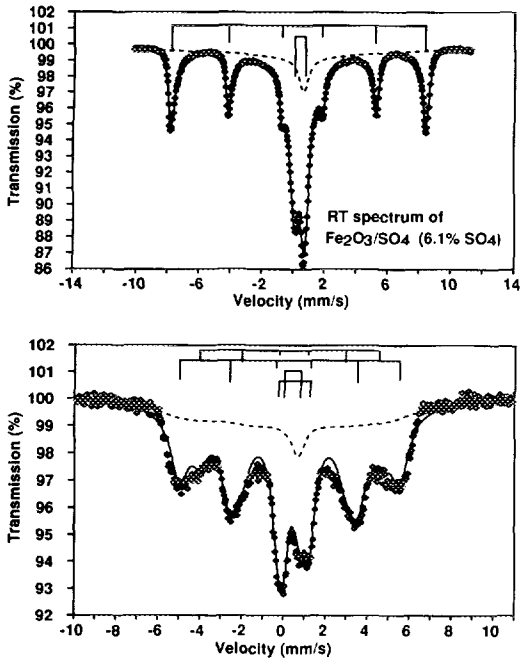

FIG. 2. Examples of some superparamagnetic fits.

Fe_2O_3 structure) and a lignite coal, ion exchanged with $FeCl_2$ (α-FeOOH structure). It can be seen that these spectra have different relative amounts of the three components. The areas under each of the components (magnetic, quadrupole, and spm) are calculated numerically by the program and used to determine the relative percentages of total iron contributing to the different components. Appropriate corrections in the peak areas for absorber thickness are taken into account by the program.

To determine size distributions, the samples are run at several temperatures. The spectrum at each temperature is analyzed using the model mentioned above. The percentage of iron contributing to the magnetic hyperfine component is taken as the percentage of iron contained in particles of volume greater than the critical volume V_c at that temperature, given by Eq. (3). Figure 4 shows the results using this approach for a catalyst consisting of Fe_2O_3 deposited on carbon (*17*). The top half of Fig. 4 shows the Mössbauer magnetic percentage for this catalyst as a function of temperature. Then, using Eq. (3) and assuming spherical particles, a critical diameter can be derived for each temperature, leading to the size distribution shown in the bottom half of Fig. 4.

The concept of assigning the percentage of iron contributing to the magnetic hyperfine spectra to particles exceeding a critical volume is similar to the approach of Kundig *et al.* (*8*). However, the incorporation of a spm relaxation component enables the magnetic and quadrupole components to be more accurately fit, leading to a correct magnetic percentage, rather than one which artificially incorporates a substantial amount of the spm spectral absorption.

Size distributions derived by this method are shown for a number of as-prepared and as-dispersed catalyst in Fig. 5. Note that the horizontal axes here and in Figure 4 are divided into equal increments corresponding to the critical particle diameter for each temperature (Eq. (3)) and are therefore not linear. The sulfated Fe_2O_3 catalysts (Fig. 5,

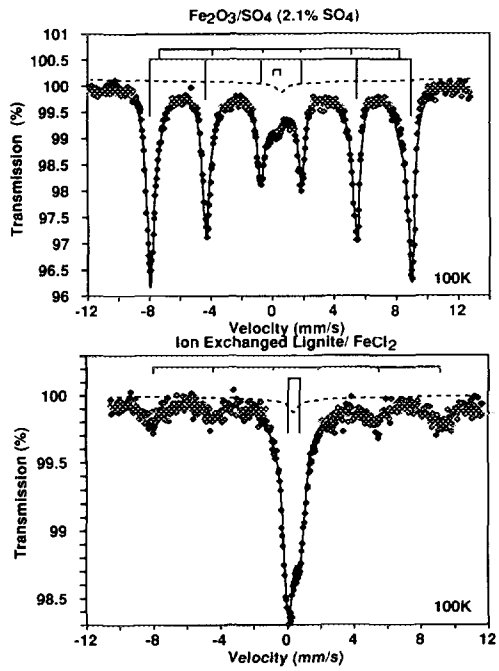

FIG. 3. Superparamagnetic fits of some samples at 100 K.

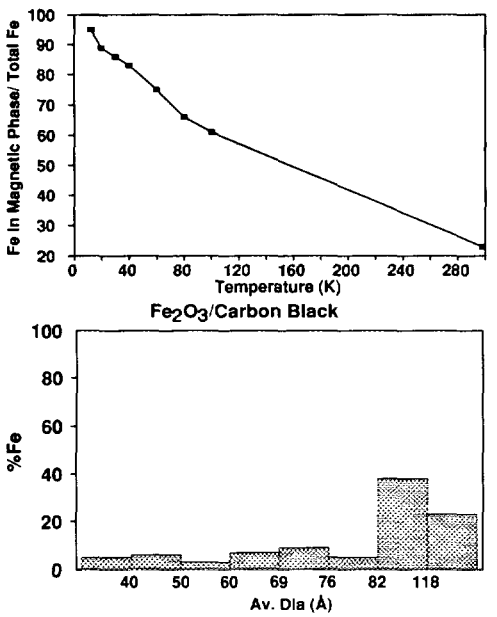

FIG. 4. Magnetic percentage vs temperature for Fe_2O_3 on carbon black and resulting size distributions.

top) were prepared at the University of Pittsburgh and have been demonstrated to have excellent activity for DCL (*4*). The $FeOOH/SO_4$ catalyst was prepared in the same investigation (*4*), but was not subjected to calcining. The 30-Å FeOOH catalyst was provided by Mach I, Inc. (*18*). As discussed elsewhere (*27, 31*), this catalyst exhibits many interesting properties, including a markedly decreased Mössbauer recoilless fraction. For current purposes, however, we merely note that the size distribution for this sample in Fig. 5 is in good agreement with TEM measurements (*31*). The size distributions shown in the lower part of Fig. 5 are somewhat different, as they represent iron incorporated into a low-rank coal (Beulah lignite) by cation exchange. As discussed elsewhere (*32*), such cation-exchanged iron constitutes an excellent DCL catalyst. The structure of the cation-exchanged iron is found to be FeOOH and, as seen, the size distributions are bimodal. Moreover, it should be noted that part of the iron included in particles in the coal that are <28 Å diameter may in fact be molecularly dispersed and bonded to the oxygen anions of carboxyl groups in the coal.

Further advantages of this fitting model is that it does not assume any kind of standard distribution, such as the often used log normal distribution (*29*), but numerically fits the data itself as a combination of magnetic, quadrupole and spm components. In case of pure oxides and oxyhydroxides, this new method of fitting the Mössbauer spectrum can directly give an estimate of the size-distribution profile by simply running the sample at one temperature, provided that the sample exhibits all three components at that temperature. Figure 6 shows some examples of the size distribution obtained from a single-temperature spectrum. The top part of Fig. 6 shows the size distribution of two sulfated Fe_2O_3 catalysts from their 50- and 100-K spectrum, respectively, and the bottom part shows the size distribution of an Fe-acetate ion-exchanged lignite coal run at room temperature and an $FeCl_2$ ion-exchanged lignite coal run at 100 K. A comparison with Fig. 5 shows that although the size distribution obtained from a single-temperature spectrum is a rather rough one, it still gives the correct estimation.

Clearly, there is some ambiguity with this approximation. For particles that are only a few nanometers in diameter, there will always be several magnetic components due to the fact that iron spins on or near the particle surface are exchange coupled to fewer neighboring iron spins than those in the interior of the particles. The interior iron atoms will therefore exhibit hyperfine fields closer to the bulk value than the surface atoms. For iron chemically impregnated or cation exchanged into the coal, there may be several inequivalent atomic envirionments for the iron contributing to both the quadrupole and magnetic hyperfine spectra. Additionally, there will be other iron-bearing species present in the coal, several of which (siderite, szomolnokite, jarosite) are magnetically ordered at low temperatures

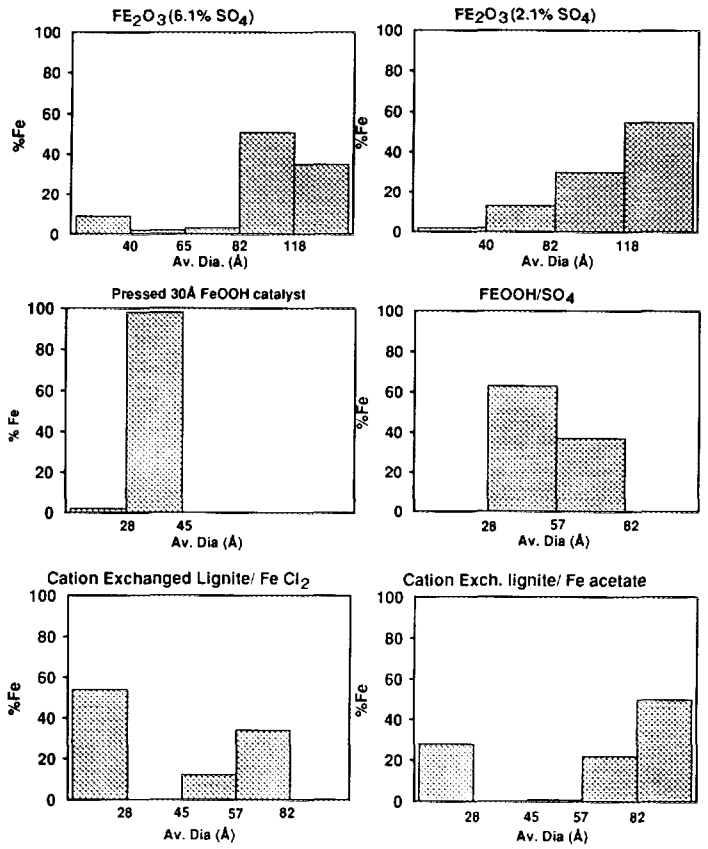

FIG. 5. Size distributions for as-prepared iron-based catalysts determined from their superparamagnetic Mössbauer spectra.

(*15*). All of these factors complicate the spectra and make it somewhat more difficult to accurately derive the correct magnetic percentage to be used in conjunction with Eq. (4) to determine size distributions. Nevertheless, the derived percentages are believed to have an error of not more than 10–20% of their true values. Regarding the use of a mean diameter for the size classification, it is obvious that this should be viewed as a dimension characteristic of the particle size rather than a true diameter, since the particles exhibit a variety of shapes. Despite these reservations, it is worth noting that mean diameters and size distributions derived by other methods such as X-ray diffraction (XRD) line broadening (*4*) and magnetic measurements (*30*) are subject to the same reservations and limitations.

Comparison to Other Methods

It is of interest to compare the size distributions detained by Mössbauer spectroscopy to those determined by other methods. As noted above, the Mach I FeOOH catalyst was investigated by STEM (*27*) and found to have a relatively tight size distribution with a mean diameter of approximately 30 Å. The Mössbauer size distribution for this sample (Fig. 5) is in good agreement with the STEM results. For the sulfated Fe_2O_3 sample containing 6.1% SO_4^{2-}, XRD, TEM, and SQUID magnetometry data on particle

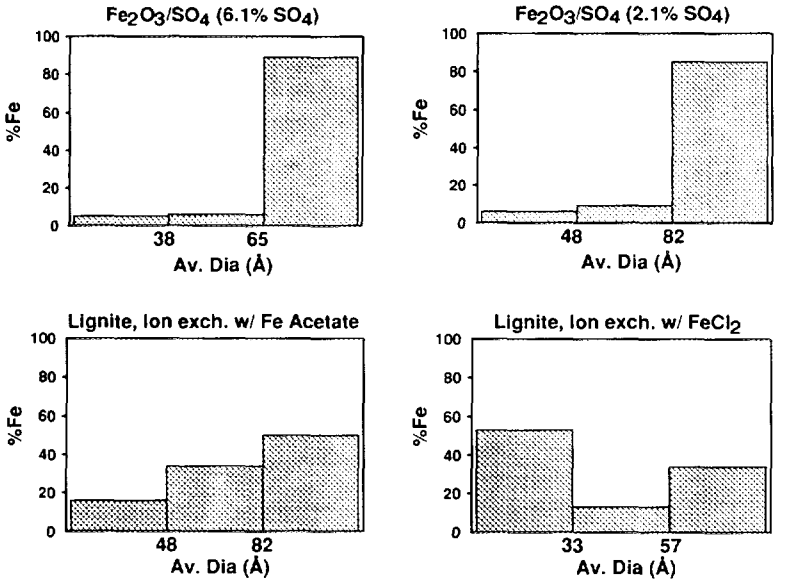

FIG. 6. Some examples of size distribution calculated from a single-temperature spectrum.

sizes are also available which allows us to compare the current technique to the other existing techniques. For this sample, the XRD line broadening gives a mean diameter of 120 Å (*4*). A particle-size distribution derived from TEM micrographs (*27*) shows particle dimensions ranging from 25 to 300 Å, with a mean diameter of approximately 140 Å. The SQUID magnetometry data (*30*) on this sample were interpreted using a log-normal size distribution and produced a size distribution ranging from 70 to 270 Å, peaking at about 110–130 Å. The particle dimensions shown in Fig. 5 derived from the current technique show a peak at 80–120 Å. It should be noted, however, that the size distribution above 118 Å, the critical diameter for α-Fe_2O_3 at room temperature, is not really defined by the Mössbauer data other than specifying the percentage of particles exceeding that diameter, since this is the highest temperature at which spectra were obtained in this study. Since a number of approximations are involved in the interpretation of all of these types of data, it is encouraging that the Mössbauer-determined size distributions agree reasonably well with the size information obtained by SQUID magnetometry, STEM, and XRD.

SUMMARY

Mössbauer spectroscopy has been used to derive the size dispersion of a variety of ultrafine iron-based direct coal liquefaction catalysts which show superparamagnetic (spm) behavior. It was shown that the relaxation spectra of these catalysts could be analyzed to yield particle volumes, and that such analyses of spectra obtained at several temperatures provide size distributions for the catalyst particles. A novel method of fitting the spectra was developed, in which the larger particles were represented by magnetic hyperfine components, the smaller particles by quadrupole doublets, and particles of intermediate volume by an spm relaxation spectrum. The size distributions were determined by measuring the magnetic hyperfine percentage as a function of temperature, each temperature corresponding to a critical diameter required for a magnetic Mössbauer spectrum. Comparison of the size distributions determined in this manner to size information obtained from TEM,

SQUID magnetometry, and XRD gave reasonable agreement. Moreover, it was demonstrated that it is possible to obtain a rough estimate of the size distribution from a spectrum obtained at a single temperature, provided the spectrum exhibits a reasonable amount of all three spectral components (magnetic, quadrupole, and spm). Future research will concentrate on the agglomeration, growth, and transformation of these iron-based catalysts during direct coal liquefaction.

ACKNOWLEDGMENTS

This research was supported by the U.S. Department of Energy under DoE Contract DE-FC22-90PC90029 as part of the research program of the Consortium for Fossil Fuel Liquefaction Science. The authors express their appreciation to a number of colleagues who provided samples for this investigation: Irving Wender and Vivek Pradhan of the University of Pittsburgh, Malvina Farcasiu of the U.S. DoE Pittsburgh Energy Technology Center, Bernard M. Kosowsky of Mach I, Inc., and Mehdi Taghiei of the University of Kentucky.

REFERENCES

1. Suzuki, T., Yamada, O., Takehashi, Y., and Watanabe, Y., *Fuel Process. Technol.* **10,** 33 (1985).
2. Tanaba, K., Yamaguchi, Y., Hattori, H., Sanada, Y., and Yokoyama, S., *Fuel Process. Technol.* **8,** 117 (1984).
3. Herrick, D. E., Tierney, J. W., Wender, I., Huffman, G. P., and Huggins, F. E., *Energy Fuels,* **4,** 231 (1991).
4. Pradhan, V. R., Tierney, J. W., Wender, I., and Huffman, G. P., *Fuels* **5,** 497 (1991).
5. Cook, P. S., Cashion, J. D., *Fuel,* **66,** 661 (1987).
6. Huffman, G. P., Huggins, F. E., Ganguly, B., Shah, N., Taghiei, M. M., Hager, G. T., *in* "Proceedings, 1991 International Conference on Coal Science, Newcastle, England, p. 826. *in* Int. Energy Agency, Butterworth–Heineman Ltd., London, 1991.
7. Shinjo, Teruya, *J. Phys. Soc. Jpn* **21**(5), 917 (1966).
8. Kundig, W., Bommel, H., Constabaris, G., and Lindquist, R. H., *Phys. Rev.* **142,** 327 (1966).
9. Van der Kraan, A. M., *Phys. Status Solidi A* **18,** 215 (1973).
10. Vertes, A., Huang, T. C., Van der Hoff, J. W., Lazar, K., Bennetech, M., and Reiff, W., *Radiochem. Radioanal. Lett.* **59**(5–6), 307 (1983).
11. Van der Kraan, A. M., Thesis (1972).
12. Rodmacq, B., *J. Phys. Chem. Solids* **45**(11–12), 1119 (1984).
13. Roggwiller, P., and Kundig, W., *Solid State Commun.* **12,** 901 (1973).
14. Huffman, G. P., and Huggins, F. E., *Fuel* **47,** 592 (1978).
15. Huggins, F. E., and Huffman, G. P., *in* "Mössbauer Analysis of the Iron-Bearing Phases in Coal, Coke and Ash, Analytical Methods for Coal and Coal Products" (C. Karr, Jr., Ed.), Vol III, 371. Academic Press, New York, 1979.
16. Huffman, G. P., *Chemtech* **10,** 504 (1980).
17. Sample provided by Malvina Farcasiu, U.S. DOE Pittsburgh Energy Technology Center, Pittsburgh, PA.
18. "Nanocat" Superfine Iron Oxide, prepared by Mach I, Inc., 340 E. Church Rd., King of Prussia, PA 19406.
19. Huffman, G. P., Ganguly, B., Taghiei, M., Huggins, F. E., and Shah, N., *Prepr. Am. Chem. Soc. Div. Fuel Chem.* **36**(2), 561 (1991).
20. Neel, L., *Rev. Mod. Phys.* **25,** 293 (1953).
21. Van der Woude, F., and Dekker, A. J., *Phys. Status Solidi* **13,** 181 (1966).
22. Blume, M., and Tjon, J. A., *Phys. Rev.* **165,** 446 (1968).
23. Wickman, H. H., "Mössbauer Effect Methodology" (I. J. Gruverman, Ed.), Vol II, p. 39. Plenum, New York, 1966.
24. Krop, K., Korecki, J., Zukrowski, J., and Karas, W., *Int. J. Magn.* **6,** 19 (1974).
25. Wehner, H. L., Ritter, G., and Wegener, H. H. F., *Phys. Lett.* **46A**(5), 333 (1974).
26. Belozerskii, G. N., and Pavlyukhin, Yu. T., *Sov. Phys. Solid State* **19**(5), 745 (1977).
27. Feng, Z., Zhao, J., Huggins, F. E., and Huffman, G. P., submitted for publication.
28. Blume, M., *Phys. Rev. Lett.* **14**(4), 96 (1965).
29. Richardson, J. J., and Desai, P., *J. Catal.* **42,** 294 (1976).
30. Ibrahim, M. M., Zhao, J., and Seehra, M. S., *J. Mater. Res.* **7,** 1856 (1992).
31. Ganguly, B., Huggins, F. E., Feng, Z., and Huffman, G. P., submitted for publication.
32. Taghiei, M. M., Huggins, F. E., Ganguly, B., and Huffman, G. P., Energy & Fuels, in press.